Intense gamma-ray source based on focused electron beams from a laser wakefield accelerator

V. Senthilkumaran,^{1, a)} D. Bailie,² K. Behm,³ J. Warwick,² G. M. Samarin,² A. Maksimchuk,³ J. Nees,³ A. G. R. Thomas,³ G. Sarri,² K. Krushelnick,³ and A. E. Hussein¹

(Dated: 14 June 2022)

Laser wakefield accelerators generate ultrashort electron bunches with the capability to produce γ -rays. Here, we produce focused LWFA electron beams using three quadrupole magnets. Electron beams are then focused into a 3 mm lead converter to generate intense, focused bremsstrahlung γ beams. Experimental results demonstrate the generation and propagation of focused γ beams to a best focus spot size of 2.3 ± 0.1 mm $\times 2.7 \pm 0.2$ mm using a copper stack calorimeter. Monte Carlo simulations conducted using GEANT4 are in good agreement with experimental results and enable detailed examination of γ -ray generation. Simulations indicate that the focused γ beams contained 2.6×10^9 photons in the range of 100 keV to 33 MeV with average energy of 6.4 MeV. A γ -ray intensity of 7×10^{10} W/cm² was estimated from simulations. The generation of focused bremsstrahlung γ -ray sources can have important applications in medical imaging applications and laboratory astrophysics experiments.

Laser wakefield acceleration (LWFA) is a compact approach for accelerating electrons in the electric fields produced by the interaction of an intense laser pulse with underdense plasma 1 . The most efficient "bubble" regime of LWFA is achieved when the laser pulse duration, t_p , is less than the plasma period $(t_p < 2\pi c/\omega_p)^{1,2}$, where ω_p is plasma frequency and occurs for normalized laser vector potential, $a_0 \gg 1$. LWFA was proposed by Tajima and Dawson in their seminal paper in 1979^1 . Since then, experimental demonstrations of the energetic electron beams $^{3-6}$ have advanced to the generation of 8 GeV electrons 7 from a centimeter-scale plasma. LWFA electron beams have ultrashort, few-femtosecond (fs) duration 8,9 with superior peak current (1–10 kA) 9,10 , narrow energy spreads of few $\%^{10}$, and minuscule transverse source sizes $(\mu m)^{11-14}$. These features make them suitable for next-generation compact, ultrafast X-ray and γ -ray sources $^{14-23}$.

The interaction of energetic LWFA electrons with a high atomic number (Z) target can be used to generate high-flux γ -rays ^{15,20,23–26}. γ -rays represent the highest energy photons in the electromagnetic spectrum, here considered as photons with a minimum energy of 10 keV. Bright γ -rays with multi-MeV energies enable greater penetration into dense materials and are desirable for numerous applications such as laboratory astrophysics²⁷, photon–photon colliders²⁸, radiotherapy²⁹, and photonuclear studies³⁰. LWFA generated γ -sources are compact^{31,32}, enabling miniaturized accelerator setups fitting in a standard-sized laboratory. However, for many of these applications, a reduction in electron beam size is desired³³. In particular, the γ -ray beams with reduced beam size can be generated by focusing of the driving electron beam and can play a crucial role in the detection of radioactive waste³⁴ and radiography of dense materials^{35,36}.

Quadrupole magnets have previously been implemented for electron beam focusing, resulting in reduced beam divergence and minimized pointing fluctuations^{37–40}. Quadrupole magnets are comprised of four magnets along with magnetization vectors^{41,42}. In this configuration, the dipoles at the system core are negated and the field magnitude is directly proportional to radial distance. Hence, electrons near the center of the quadrupole magnet will experience a weaker force. Furthermore, an electron traveling through a quadrupole magnet will defocus in one plane and focus on another.

In this Letter, we present the generation of γ beams with reduced beam profiles using focused LWFA electron beams. Firstly, E \simeq 200 MeV LWFA electron beams were focused using quadrupole magnets, resulting in improved beam pointing and stability. Electron beams were then focused into a lead (Pb) converter target for γ -ray generation. A copper (Cu) stack calorimeter enabled visualization of the spatial propagation of γ -ray beams, demonstrating the production of a γ beam of $2.3 \pm 0.1 \text{ mm} \times 2.7 \pm 0.2 \text{ mm}$ at best focus. Monte Carlo simulations using the GEANT4 code were in good agreement with experimental results in terms of beam propagation and focusing. GEANT4 simulations indicate that γ beams with an average photon energy of 6.4 MeV and $N_{ph} \simeq 2.6 \times 10^9$ photons with energy ranging from 100 keV to 33 MeV were generated. The simulated γ beam had a focused intensity of 7×10^{10} W/cm² with beam size of 2.4 mm × 2.4 mm and this was nearly 4× higher than intensity obtained using a collimated input electron beam scenario.

Experiments were conducted using the HERCULES laser facility at the University of Michigan⁴³. HERCULES is an 800 nm Ti:Sapphire laser system with a full-width-at-half-maximum (FWHM) pulse duration of ~ 35 fs. The laser had an average power of 70.5 ± 1.6 TW and was focused using an f/20 off-axis parabolic mirror to an intensity of about 1.2×10^{19} W/cm², corresponding to a normalized vector po-

¹⁾Department of Electrical and Computer Engineering, University of Alberta, Edmonton, Alberta T6G 1H9, Canada

²⁾Centre for Plasma Physics, School of Mathematics and Physics, Queen's University Belfast, BT7 1NN, Belfast United Kingdom

³⁾Gérard Mourou Center for Ultrafast Optical Science, University of Michigan, Ann Arbor, Michigan 48109, IISA

a) Electronic mail: vigneshv@ualberta.ca

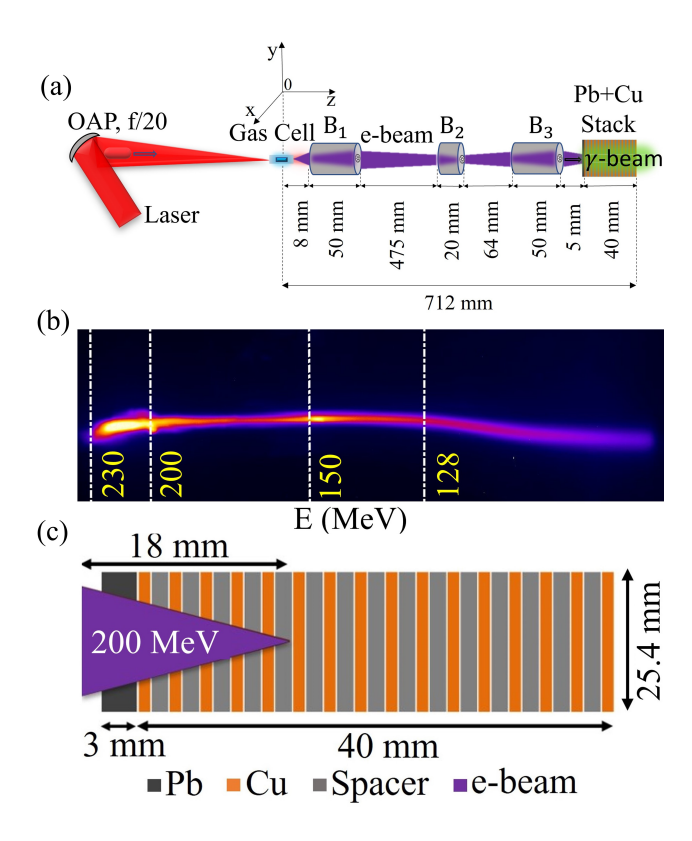


FIG. 1. (a) Schematic of the experimental setup. The HERCULES Ti:Sapphire laser beam (red) was focused into a single stage 5 mm gas cell filled with helium gas to drive an LWFA. Three quadrupole magnets (B_1, B_2, B_3) were used to focus the resultant electron beams (purple). Focused electron beams generated a γ beam (green) through interaction with a Pb converter and a Cu stack calorimeter. (b) Example electron beam imaged on a LANEX scintillating screen. (c) Schematic of the 3 mm Pb converter and Cu stack calorimeter consisting of 16 IP interwoven with Cu foils.

tential of $a_0 = 2.3$. An LWFA was driven by focusing the HERCULES beam at the entrance of single stage 5 mm gas cell filled with helium gas at pressure ranging from 5 PSIA to 8 PSIA. This corresponds to plasma electron density ranging from $0.6 \times 10^{19} \text{cm}^{-3}$ to $1 \times 10^{19} \text{cm}^{-3}$.

A schematic of the experimental setup is shown in Figure 1a). LWFA electron beams were characterized using a 0.8 T dipole magnetic spectrometer and a LANEX scintillating screen. Resultant electron beams had a maximum energy of 205 ± 25 MeV over 14 shots with a broad energy spectrum. An example electron beam is shown in Figure 1b). It is important to note that the dipole magnetic spectrometer had to be moved out of the way to implement the quadrupole magnet focusing system, therefore the LWFA electron beam could not be simultaneously characterized during focusing. Thus, the quoted electron energies are estimated from separate measurements.

To achieve focusing of the LWFA electron beam, three quadrupole magnets with 6 mm apertures were used, as shown in Figure 1a). The first quadrupole magnet ($B_1 = 1.2 \text{ T}$) was placed 8 mm away from the center of the gas cell, denoted z = 0. The second quadrupole magnet ($B_2 = 0.9 \text{ T}$) was sit-

uated 475 mm away from first quadrupole magnet, and the third quadrupole magnet ($B_3 = 1.2 \,\mathrm{T}$) was placed 64 mm away from second quadrupole magnet. B_1 and the B_3 focused (defocused) electron beam in the vertical (horizontal) axis while B_2 defocused (focused) it in the horizontal (vertical) axis. The electron beam profile was imaged at various position along the axis of laser propagation (z) using a scintillating LANEX screen and a CCD camera. The adopted configuration was found to minimise the electron beam size for $\sim 200 \,\mathrm{MeV}$. The position of this screen was varied to determine the point of best focus at $z=685 \,\mathrm{mm}$ from the back of the gas cell (i.e., $z=18 \,\mathrm{mm}$ behind from the third quadrupole magnet).

A Pb bremsstrahlung converter and a Cu stack calorimeter, depicted in Figure 1c), was used for γ -ray generation and investigation of beam propagation. A 3 mm Pb converter was placed along the laser axis at 2 mm behind the third quadrupole magnet. The Cu stack calorimeter consisted of sixteen 1 mm thick, 25.4 mm \times 25.4 mm Cu foils interwoven with image plate (IP) and separated by 1.5 mm using a cardboard frame was placed behind the Pb converter for measurements of the resultant γ beam via Cu autoradiography. The IP consisted of 100 μ m layer of luminescent material of BaFBr:Eu²⁺. The calorimeter stack, spanning 40 mm, enabled investigation of the propagation dynamics and generation of intense γ beams. Calorimetry was performed with and without the Pb converter to account for Cu self-emission.

The GEANT4 (GEometry ANd Tracking) simulation toolkit⁴⁴ was used to examine the propagation dynamics of an energetic electron beam traveling through a Pb converter and a Cu stack calorimeter. An electron beam containing $N_e = 10^8$ electrons with an energy of 200 MeV propagating in vacuum and entering a 3 mm Pb block and 40 mm Cu + IP stack was simulated, matching the experimental geometry in Figure 1c). Photons of energies above 100 keV were recorded. Information pertaining to energy of simulated photons, deposited energies and number of simulated photons were collected by multi-functional detectors placed inside the geometry of the Cu stack for comparison with experimental results on the IP. Analysis of energy transfer to secondaries and energy deposition was conducted to understand the overall energy contribution from each materials (Pb, Cu and IP). The energy contribution of the IP was found to be negligible $(E_{IP\ contribution}/E_{Pb+Cu\ stack\ contribution}=0.003).$

The properties of LWFA electron beams with and without the quadrupole magnet system are shown in Figure 2. Using the quadrupole magnet system, the electron beam was focused to $1.4 \pm 0.4 \times 1.1 \pm 0.3$ mm (FWHM in $x \times$ FWHM in y) at z = 685 mm from the back of the gas cell (Figure 2a)). Without the magnet system, the beam size at z = 533 mm was $3.2 \pm 0.4 \times 2.7 \pm 0.5$ mm (x-axis \times y-axis), after which the beam would continue to diverge³⁸.

The stability of the electron beam was characterized by the variation in the location of the center of the electron beam. Electron beam stability improved from an average of 2.8 ± 1.4 mrad, $(3.0 \pm 0.6$ mrad FWHM in x and 2.5 ± 0.5 mrad FWHM in y) without quadrupole magnets to 0.8 ± 0.3 mrad (1.0 ± 0.3) mrad FWHM in x and x

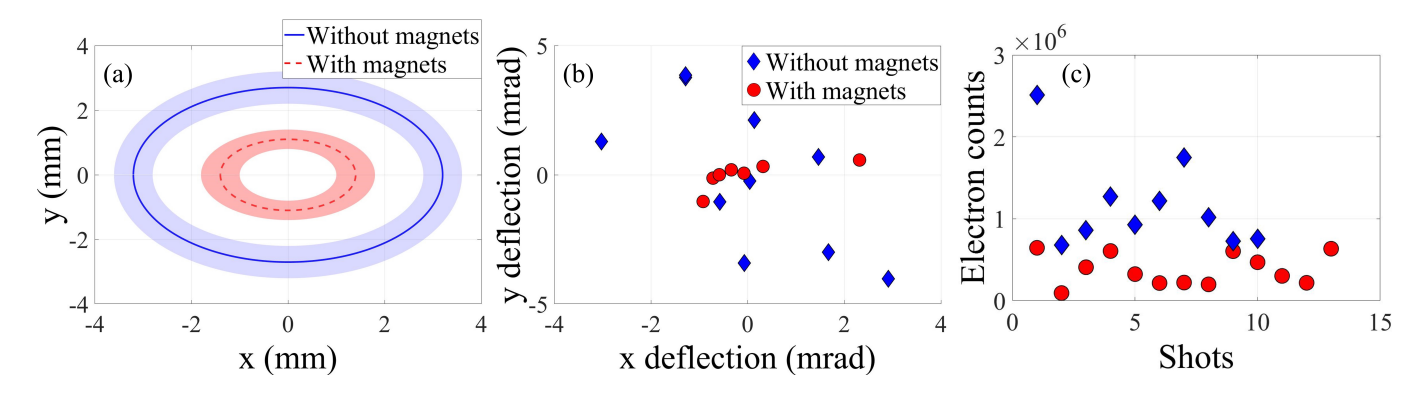


FIG. 2. Comparison of (a) electron beam transverse profile (lines denote mean and shaded regions denote standard deviation over 10 shots, (b) shot-to-shot pointing stability and (c) background subtracted electron counts (arb. u.), with and without the triplet quadrupole magnet system.

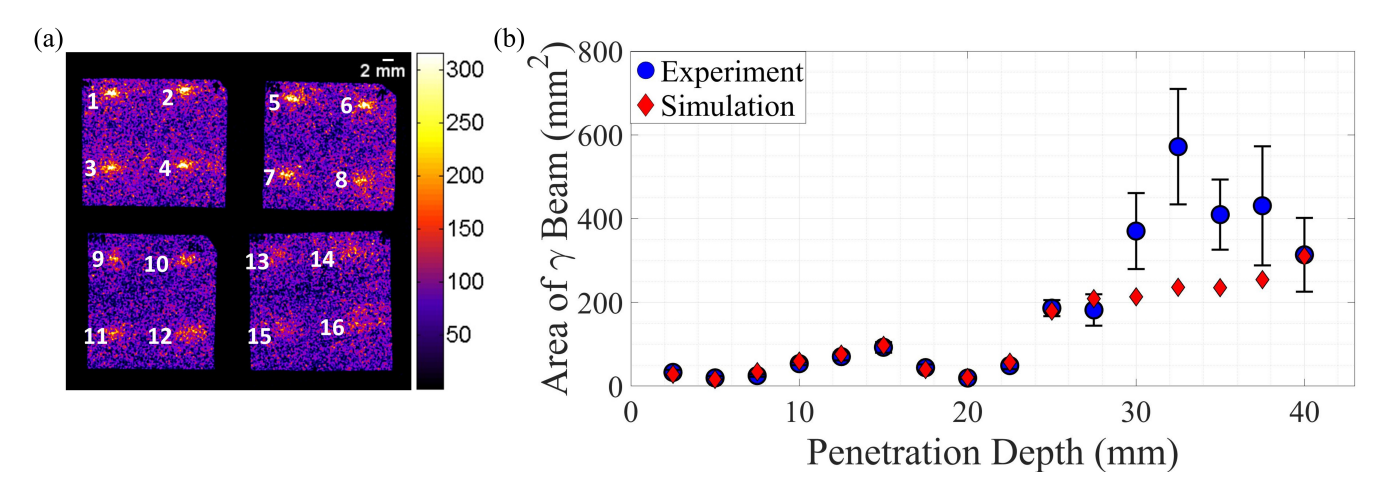


FIG. 3. (a) Raw Cu autoradiography data from each IP, demonstrating γ -ray generation. (b) Comparison of experimental data and GEANT4 simulation of the γ beam profile as a function of penetration depth.

Using the quadrupole system, a reduction of counts on the scintillating LANEX screen, representing the beam charge, was observed (Figure 2c)). This is attributed to the loss of high-divergence low-energy electrons at the 6 mm magnet aperture $^{45-47}$ and low-energy electrons do not get focused well by the quadrupole magnets 40 . The mean number of counts in the electron beam over ten shots was measured to be $(3.8\pm1.9)\times10^5$ with quadrupole magnets and $(11.7\pm5.7)\times10^5$ without.

Raw IP measurements from the Cu stack calorimeter are shown in Figure 3a) at sixteen locations along the propagation axis, where '1', corresponds to the first IP, located directly behind the 3 mm Pb converter, and '16' denotes the last IP, 40 mm behind the converter. The γ beam was approximated as an ellipse with area = πxy , where x and y are the beam FWHM in each dimension. The area of the γ beam as function of penetration depth from both experiments and simulations is shown in Figure 3b). GEANT4 simulations account for beam area of γ -ray photons with energy exceeding 100 keV and variations in the beam area along the focusing geometry. Here, the focusing geometry determines the spatial distribution of the γ -ray photons along the focal volume of the Cu/IP stack. Input electron energy transferred to secondaries

which are not γ -ray photons constitute 15% of total input energy, as verified with NIST⁴⁸ and GEANT4. Thus, excellent agreement between simulations and experimental results up to penetration depths of 25 mm (Figure 3b)) i.e., at z = 692 mm from the back of the gas cell, indicate that the intense spots recorded on the IPs can reasonably be considered as capturing the spatial propagation of γ -rays. Variations in beam area beyond penetration depths of 25 mm may be attributed to secondary radiation showers and greater uncertainty in estimating beam area experimentally.

From calorimetry measurements, it was found that the γ beam came to focus at a penetration depth of 20 mm (z=687 mm from the back of the gas cell), closely matching the location of best focus of the LWFA electron beam (z=685 mm). At best focus, the γ beam size was 2.3 ± 0.1 mm \times 2.7 ± 0.2 mm (19.3 ± 2.5 mm² area) in experiments, as compared to 2.4 mm \times 2.4 mm (18 mm² area) from simulations. More than four-fold increase in beam area was observed after a penetration depth of 25 mm in both simulations and experiments, indicating significant beam scattering. The experimentally observed trends in γ beam propagation and focusing were in excellent agreement with GEANT4 simulations.

From GEANT4 simulations, a total of photons N_{ph} =

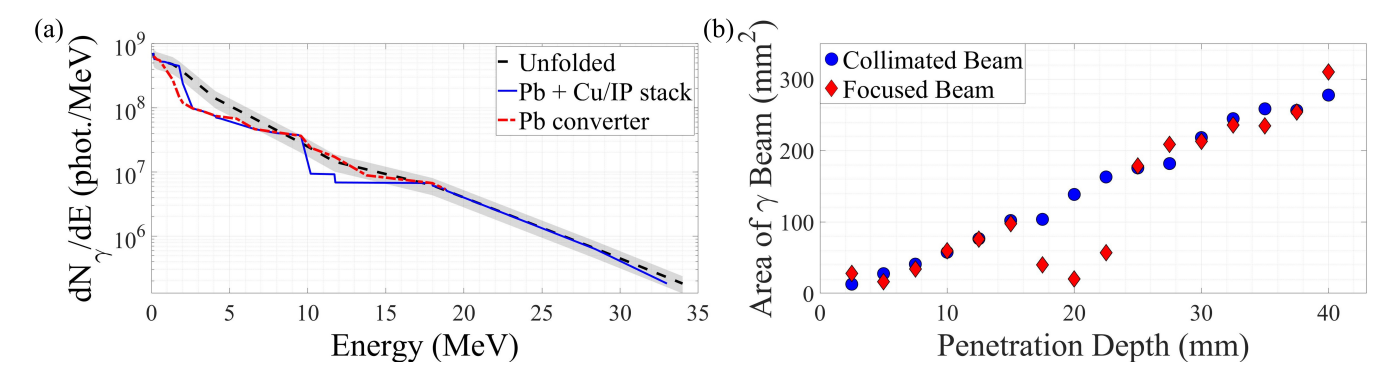


FIG. 4. (a) Spectrum of γ -rays simulated in GEANT4 for both the Pb+Cu/IP stack and Pb converter respectively, as well as the unfolded spectrum, where the gray shaded area represents the uncertainty of unfolding. (b) Comparison of simulated γ beam profile obtained using collimated and focusing input electron beams.

 2.6×10^9 in the range of 100 keV to 33 MeV, with an average energy of 6.4 MeV, were generated along the 40 mm interaction length, with a pulse duration of 0.5 ps. The electron-to-photon conversion efficiency^{15,49} (CE) was $N_{ph}/N_e = 26$. The spectrum of the resultant γ -rays from GEANT4 simulations (Figure 4a)) was obtained by⁵⁰:

$$\frac{dN_{\gamma}}{dE} = Rl\left(\left(1 - b + \frac{1}{rE}\right)e^{-rE} + \left(b - \frac{E_0}{E} - \frac{1}{rE}\right)e^{-rE_0}\right)$$

where dN_{γ}/dE is the number of bremsstrahlung photons at a photon energy E>100 keV recorded from GEANT4, l is thickness of Cu foils in the 40 mm stack calorimeter, E_0 is the electron energy of $E_0 \simeq 200$ MeV, $b \approx 0.83$ is a dimensionless constant, r is a fitting parameter with dimension of MeV⁻¹, used for estimating γ -ray spectrum, where $r \approx 1.2$ MeV⁻¹ for 100 keV < E < 2 MeV, and $r \approx 0.25$ MeV⁻¹ for E > 2 MeV and R is a group of constants constituting the atomic density, n_a , and atomic number, Z, of Pb and Cu, as well as fitting parameters, such that $R = Cn_aZ^2r^{-1}$, where C $\approx 1.1 \times 10^{-18}$ cm².

The 3 mm Pb converter was found to produce 62% of total photons above 100 keV, with the remaining 38% originating from the subsequent Cu stacks. The electron-to-photon conversion efficiency in the Pb converter alone was 15, producing bremsstrahlung photons averaging 4 MeV in the range of 100 keV to 18 MeV. At best focus, the intensity of the focused γ beam in the Pb + Cu stack was nearly 7 times higher than achieved in Pb alone. At this location, the gamma beam area was 8 mm² from the Pb converter alone, versus 18 mm² in the Pb + Cu stack; the Cu stack increased the beam size and number of photons by enabling more scattering events. It is important to note that the focusing geometry was preserved in this comparison, therefore the location of best focus of the electron and associated gamma beam was not within the Pb converter, but rather at z = 687 mm from the back of the gas cell, behind the 3 mm Pb converter. The simulated spectrum of the bremsstrahlung source produced from the Pb converter is also given in Figure 4a).

The γ -ray spectrum from experimental measurements was

reconstructed by using an unfolding algorithm⁵¹:

$$E_{dep,j} = \sum_{i=1}^{n} P(E_{dep,j}, E_{in,i}) \times f(E_{in,i})$$
 (2)

where $E_{dep,j}$ represents energy deposition per layer of the stack calorimeter, $P(E_{dep,j}, E_{in,i})$ is a response matrix that connects the incident energy spectrum to the energy deposited on the detector, and $f(E_{in,i})$ is the binned energy spectrum. The response matrix was obtained from GEANT4 simulations for photons ranging from 100 keV to 200 MeV using 650 energy bins; for unfolding up to 50 MeV, 100 keV energy bins were used, subsequently 1 MeV bins were used for beyond 50 MeV. The bremsstrahlung Findlay prior⁵² function was used as the initial assumed energy spectrum $f(E_{in.i})$. The unfolding algorithm was implemented in an iterative manner, with the measured energy deposition from the image plate conversion IP from PSL to MeV⁵³ compared to energy deposition from unfolding algorithm using least squares minimization in each step. Finally, the spectrum due to energy deposition was calculated using equation 2. The unfolded γ -ray spectrum shown in Figure 4a) is in close agreement with the GEANT4 simulated γ -ray spectrum, where the estimated number of photons was $2.5 \pm 0.2 \times 10^9$ in the range of 100 keV to 34 MeV with average energy of 6.1 ± 0.5 MeV, whereas in the GEANT4 simulation, number of photons was 2.6×10^9 in the range of 100 keV to 33 MeV, with an average energy of 6.4 MeV.

The propagation and intensity of a γ beam driven by a collimated electron beam was also simulated in GEANT4. Figure 4b) shows a comparison between γ beam profile using (3 × 3) mm electron beam focusing to approximately (1.4 × 1.1) mm and a collimated electron beam of (3 × 3) mm. Using a collimated input electron beam, the size of the γ beam was found to increase linearly with propagation distance. The number of photons generated using a focused or collimated beam was nearly same ($N_{ph\ focused} = 2.6 \times 10^9$, $N_{ph\ collimated} = 2.5 \times 10^9$), however, at the location of best focus (z = 687 mm from the back of the gas cell), the γ -ray intensity for the focused case was nearly 4× higher than the collimated case ($I_{focused} = 7 \times 10^{10}$ W/cm² in a beam area of 18 mm² versus $I_{collimated} = 1.8 \times 10^{10}$ W/cm² in a beam area

of 130 mm^2).

The peak brilliance of the focused γ -ray source was $\sim 3 \times 10^{17}$ photons s $^{-1}$ mm $^{-2}$ mrad $^{-2}$ 0.1% BW . This source is comparable to brilliance of other bremsstrahlung radiation sources ($\sim 2 \times 10^{17}$ photons s $^{-1}$ mm $^{-2}$ mrad $^{-2}$ 0.1% BW from Giulietti *et al.* 30 and $\sim 1 \times 10^{17}$ photons s $^{-1}$ mm $^{-2}$ mrad $^{-2}$ 0.1% BW from Glinec *et al.* 35 with 'Ta' target in both reports) discussed in the literature 17,54 .

In this work, a system of three quadrupole magnets was used to generate focused LWFA electron beams, demonstrating improved beam stability and pointing. This system was subsequently used to focus the electron beam into a 3 mm Pb converter and a Cu stack calorimeter for generation and diagnosis of resultant bremsstrahlung γ -rays. The Cu stack calorimeter enabled visualization of the spatial propagation of γ -ray beams, demonstrating the production of γ beam of $2.3 \pm 0.1 \; \mathrm{mm} \times 2.7 \pm 0.2 \; \mathrm{mm}$ at best focus. The location of best focus of the γ beam was in close agreement with best focus of the electron beam to (1.4×1.1) mm. Experimental trends were well reproduced in GEANT4 simulations, in which 2.6×10^9 photons with an average energy of 6.4 MeV in the range of 100 keV to 33 MeV were focused to an intensity of 7×10^{10} W/cm² while simulated γ -ray pulse duration was 0.5 ps, with peak brilliance of $\sim 3 \times 10^{17}$ photons s⁻¹ mm⁻² mrad⁻² 0.1% BW.

This demonstration of intense, focused γ beams produced from an LWFA has significant potential in a variety of applications, including radiography of dense materials^{35,36}, experimental studies of extreme astrophysical environments 15,27, the detection of illegal nuclear materials⁵⁵ and radioactive tracers in medical imaging^{34,35} and the disposal of nuclear waste 15,55,56 . Specifically, the γ -ray source of present work may be suitable for high-resolution γ -ray radiography which requires γ -ray photons with energies up to 10 MeV and fewmm resolution¹⁴. These results are also relevant to laser driven radioisotope production systems, requiring γ -rays between 15 and 25 MeV¹⁵. Additionally, the application of focused LWFA electron beams with a high-Z converter could be employed to generate positron beams through the Bethe-Heitler mechanism for the study of neutral electron-positron plasma^{57,58} dynamics to replicate γ -ray bursts^{59,60} in the laboratory 54,61 . The achievement of narrowband energy γ sources using filters¹⁵ or crystal lenses⁶² could further optimize these sources for many industry relevant applications.

While quadrupole magnets were employed here for electron beam focusing, an active plasma lens may provide an alternative with the capability to provide a more compact arrangement with tunable focusing ability⁶³ and reduced dependence of focal length on electron energy⁶⁴. However, active plasma lenses suffer from aberrations triggered by radially nonuniform focusing fields, potentially degrading beam quality and beam focusing trajectory, and could also be subject to interference from the plasma wakefield⁶⁵.

V. Senthilkumaran and A.E. Hussein acknowledge support from the Natural Sciences and Engineering Research Council of Canada (Grant No.: RGPIN-2021-04373) and the Alberta Graduate Excellence Scholarship. A. G. R. Thomas acknowledges support from National Science Foundation (Grant

No.: 2108075). G. Sarri wishes to acknowledge support from Engineering and Physical Sciences Research Council (Grant No.: EP/N027175/1 and EP/N022696/1). K. Krushelnick acknowledges support from US DOE grant (Grant No.: DE-SC0022109) for the experimental work.

The data that support the findings of this study are available from the corresponding author upon reasonable request.

- ¹T. Tajima and J. M. Dawson, "Laser electron accelerator," Phys. Rev. Lett. **43**, 267 (1979).
- ²E. Esarey, C. B. Schroeder, and W. P. Leemans, "Physics of laser-driven plasma-based electron accelerators," Rev. Mod. Phys. **81**, 1229–1285 (2009).
- ³A. Modena, Z. Najmudin, A. E. Dangor, C. E. Clayton, K. A. Marsh, C. Joshi, V. Malka, C. B. Darrow, C. Danson, D. Neely, and F. N. Walsh, "Electron acceleration from the breaking of relativistic plasma waves," Nature 377, 606–608 (1995).
- ⁴J. Faure, Y. Glinec, A. Pukhov, S. Kiselev, S. Gordienko, E. Lefebvre, J.-P. Rousseau, F. Burgy, and V. Malka, "A laser–plasma accelerator producing monoenergetic electron beams," Nature 431, 541–544 (2004).
- ⁵C. Geddes, C. Toth, J. Van Tilborg, E. Esarey, C. Schroeder, D. Bruhwiler, C. Nieter, J. Cary, and W. Leemans, "High-quality electron beams from a laser wakefield accelerator using plasma-channel guiding," Nature 431, 538–541 (2004).
- ⁶S. P. D. Mangles, C. D. Murphy, Z. Najmudin, A. G. R. Thomas, J. L. Collier, A. E. Dangor, E. J. Divall, P. S. Foster, J. G. Gallacher, C. J. Hooker, D. A. Jaroszynski, A. J. Langley, W. B. Mori, P. A. Norreys, F. S. Tsung, R. Viskup, B. R. Walton, and K. Krushelnick, "Monoenergetic beams of relativistic electrons from intense laser–plasma interactions," Nature 431, 535–538 (2004).
- ⁷A. J. Gonsalves, K. Nakamura, J. Daniels, C. Benedetti, C. Pieronek, T. C. H. De Raadt, S. Steinke, J. H. Bin, S. S. Bulanov, J. Van Tilborg, C. G. R. Geddes, C. B. Schroeder, C. Toth, E. Esarey, K. Swanson, L. Fan-Chiang, G. Bagdasarov, N. Bobrova, V. Gasilov, G. Korn, P. Sasorov, and W. P. Leemans, "Petawatt laser guiding and electron beam acceleration to 8 GeV in a laser-heated capillary discharge waveguide," Phys. Rev. Lett. 122, 084801 (2019).
- ⁸A. Buck, M. Nicolai, K. Schmid, C. M. Sears, A. Sävert, J. M. Mikhailova, F. Krausz, M. C. Kaluza, and L. Veisz, "Real-time observation of laser-driven electron acceleration," Nat. Phys. 7, 543–548 (2011).
- ⁹O. Lundh, J. Lim, C. Rechatin, L. Ammoura, A. Ben-Ismaïl, X. Davoine, G. Gallot, J.-P. Goddet, E. Lefebvre, V. Malka, and J. Faure, "Few femtosecond, few kiloampere electron bunch produced by a laser–plasma accelerator," Nat. Phys. **7**, 219–222 (2011).
- ¹⁰S. M. Wiggins, R. C. Issac, G. H. Welsh, E. Brunetti, R. P. Shanks, M. P. Anania, S. Cipiccia, G. G. Manahan, C. Aniculaesei, B. Ersfeld, M. R. Islam, R. T. L. Burgess, G. Vieux, W. A. Gillespie, A. M. MacLeod, S. B. van der Geer, M. J. de Loos, and D. A. Jaroszynski, "High quality electron beams from a laser wakefield accelerator," Plasma Phys. Controlled Fusion 52, 124032 (2010).
- ¹¹ A. G. Khachatryan, F. A. Van Goor, K.-J. Boller, A. J. W. Reitsma, and D. A. Jaroszynski, "Extremely short relativistic-electron-bunch generation in the laser wakefield via novel bunch injection scheme," Phys. Rev. ST Accel. Beams 7, 121301 (2004).
- ¹² A. Rousse, K. T. Phuoc, R. Shah, A. Pukhov, E. Lefebvre, V. Malka, S. Kiselev, F. Burgy, J.-P. Rousseau, D. Umstadter, and D. Hulin, "Production of a keV X-ray beam from synchrotron radiation in relativistic laser-plasma interaction," Phys. Rev. Lett. 93, 135005 (2004).
- ¹³S. Kneip, C. McGuffey, J. L. Martins, S. Martins, C. Bellei, V. Chvykov, F. Dollar, R. Fonseca, C. Huntington, G. Kalintchenko, A. Maksimchuk, S. P. D. Mangles, T. Matsuoka, S. R. Nagel, C. A. J. Palmer, J. Schreiber, K. Ta Phuoc, A. G. R. Thomas, V. Yanovsky, L. O. Silva, K. Krushelnick, and Z. Najmudin, "Bright spatially coherent synchrotron X-rays from a table-top source," Nat. Phys. 6, 980–983 (2010).
- ¹⁴F. Albert and A. G. R. Thomas, "Applications of laser wakefield accelerator-based light sources," Plasma Phys. Controlled Fusion 58, 103001 (2016).
- ¹⁵S. Cipiccia, S. M. Wiggins, R. P. Shanks, M. R. Islam, G. Vieux, R. C. Issac, E. Brunetti, B. Ersfeld, G. H. Welsh, M. P. Anania, D. Maneuski, N. R. C. Lemos, R. A. Bendoyro, P. P. Rajeev, P. Foster, N. Bourgeois, T. P. A. Ib-

- botson, P. A. Walker, V. O. Shea, J. M. Dias, and D. A. Jaroszynski, "A tuneable ultra-compact high-power, ultra-short pulsed, bright gamma-ray source based on bremsstrahlung radiation from laser-plasma accelerated electrons," J. Appl. Phys. 111, 063302 (2012).
- ¹⁶S. Chen, N. D. Powers, I. Ghebregziabher, C. M. Maharjan, C. Liu, G. Golovin, S. Banerjee, J. Zhang, N. Cunningham, A. Moorti, S. Clarke, S. Pozzi, and D. P. Umstadter, "MeV-energy X rays from inverse Compton scattering with laser-wakefield accelerated electrons," Phys. Rev. Lett. 110, 155003 (2013).
- ¹⁷G. Sarri, D. J. Corvan, W. Schumaker, J. M. Cole, A. Di Piazza, H. Ahmed, C. Harvey, C. H. Keitel, K. Krushelnick, S. P. D. Mangles, Z. Najmudin, D. Symes, A. G. R. Thomas, M. Yeung, Z. Zhao, and M. Zepf, "Ultrahigh brilliance multi-mev γ-ray beams from nonlinear relativistic thomson scattering," Phys. Rev. Lett. 113, 224801 (2014).
- ¹⁸D. J. Stark, T. Toncian, and A. V. Arefiev, "Enhanced multi-MeV photon emission by a laser-driven electron beam in a self-generated magnetic field," Phys. Rev. Lett. 116, 185003 (2016).
- ¹⁹J. M. Cole, D. R. Symes, N. C. Lopes, J. C. Wood, K. Poder, S. Alatabi, S. W. Botchway, P. S. Foster, S. Gratton, S. Johnson, C. Kamperidis, O. Kononenko, M. De Lazzari, C. A. J. Palmer, D. Rusby, J. Sanderson, M. Sandholzer, G. Sarri, Z. Szoke-Kovacs, L. Teboul, J. M. Thompson, J. R. Warwick, H. Westerberg, M. A. Hill, D. P. Norris, S. P. D. Mangles, and Z. Najmudin, "High-resolution μCT of a mouse embryo using a compact laser-driven X-ray betatron source," Proc. Natl. Acad. Sci. 115, 6335–6340 (2018).
- ²⁰N. Lemos, F. Albert, J. L. Shaw, D. Papp, R. Polanek, P. King, A. L. Milder, K. A. Marsh, A. Pak, B. B. Pollock, B. M. Hegelich, J. D. Moody, J. Park, R. Tommasini, G. J. Williams, H. Chen, and C. Joshi, "Bremsstrahlung hard x-ray source driven by an electron beam from a self-modulated laser wakefield accelerator," Plasma Phys. Controlled Fusion 60, 054008 (2018).

²¹T. W. Huang, C. M. Kim, C. T. Zhou, M. H. Cho, K. Nakajima, C. M. Ryu, S. C. Ruan, and C. H. Nam, "Highly efficient laser-driven compton gamma-ray source," New J. Phys. 21, 013008 (2019).

- ²²A. E. Hussein, N. Senabulya, Y. Ma, M. J. V. Streeter, B. Kettle, S. J. D. Dann, F. Albert, N. Bourgeois, S. Cipiccia, J. M. Cole, O. Finlay, E. Gerstmayr, I. Gallardo González, A. Higginbotham, D. A. Jaroszynski, K. Falk, K. Krushelnick, N. Lemos, N. C. Lopes, C. Lumsdon, O. Lundh, S. P. D. Mangles, Z. Najmudin, P. P. Rajeev, C. M. Schlepütz, M. Shahzad, M. Smid, R. Spesyvtsev, D. R. Symes, G. Vieux, L. Willingale, J. C. Wood, A. J. Shahani, and A. G. R. Thomas, "Laser-wakefield accelerators for high-resolution X-ray imaging of complex microstructures," Sci. Rep. 9, 1–13 (2019).
- ²³C. I. D. Underwood, C. D. Baird, C. D. Murphy, C. D. Armstrong, C. Thornton, O. J. Finlay, M. J. V. Streeter, M. P. Selwood, N. Brierley, S. Cipiccia, J.-N. Gruse, P. McKenna, Z. Najmudin, D. Neely, D. Rusby, D. R. Symes, and C. M. Brenner, "Development of control mechanisms for a laser wakefield accelerator-driven bremsstrahlung x-ray source for advanced radiographic imaging," Plasma Phys. Controlled Fusion 62, 124002 (2020).
- ²⁴W. Schumaker, G. Sarri, M. Vargas, Z. Zhao, K. Behm, V. Chvykov, B. Dromey, B. Hou, A. Maksimchuk, J. Nees, V. Yanovsky, M. Zepf, A. G. R. Thomas, and K. Krushelnick, "Measurements of high-energy radiation generation from laser-wakefield accelerated electron beams," Phys. Plasmas 21, 056704 (2014).
- ²⁵ A. Döpp, E. Guillaume, C. Thaury, A. Lifschitz, F. Sylla, J.-P. Goddet, A. Tafzi, G. Iaquanello, T. Lefrou, P. Rousseau, E. Conejero, C. Ruiz, K. Ta Phuoc, and V. Malka, "A bremsstrahlung gamma-ray source based on stable ionization injection of electrons into a laser wakefield accelerator," Nucl. Instrum. Methods Phys. Res., Sect. A 830, 515–519 (2016).
- ²⁶S. Li, B. Shen, J. Xu, T. Xu, Y. Yu, J. Li, X. Lu, C. Wang, X. Wang, X. Liang, Y. Leng, R. Li, and Z. Xu, "Ultrafast multi-MeV gamma-ray beam produced by laser-accelerated electrons," Phys. Plasmas 24, 093104 (2017).
- ²⁷S. V. Bulanov, T. Z. Esirkepov, M. Kando, J. Koga, K. Kondo, and G. Korn, "On the problems of relativistic laboratory astrophysics and fundamental physics with super powerful lasers," Plasma Phys. Rep. 41, 1–51 (2015).
- ²⁸K. Homma, K. Matsuura, and K. Nakajima, "Testing helicity-dependent $\gamma\gamma \to \gamma\gamma$ scattering in the region of MeV," Prog. Theor. Exp. Phys. **2016** (2016).
- ²⁹ K. J. Weeks, V. N. Litvinenko, and J. M. J. Madey, "The compton backscat-

- tering process and radiotherapy," Med. Phys. 24, 417-423 (1997).
- ³⁰A. Giulietti, N. Bourgeois, T. Ceccotti, X. Davoine, S. Dobosz, P. D'Oliveira, M. Galimberti, J. Galy, A. Gamucci, D. Giulietti, L. A. Gizzi, D. J. Hamilton, E. Lefebvre, L. Labate, J. R. Marquès, P. Monot, H. Popescu, F. Réau, G. Sarri, P. Tomassini, and P. Martin, "Intense γ-ray source in the giant-dipole-resonance range driven by 10-tw laser pulses," Phys. Rev. Lett. 101, 105002 (2008).
- ³¹T. E. Cowan, A. W. Hunt, T. W. Phillips, S. C. Wilks, M. D. Perry, C. Brown, W. Fountain, S. Hatchett, J. Johnson, M. H. Key, T. Parnell, D. M. Pennington, R. A. Snavely, and Y. Takahashi, "Photonuclear fission from high energy electrons from ultraintense laser-solid interactions," Phys. Rev. Lett. 84, 903–906 (2000).
- ³²K. Spohr, M. Shaw, W. Galster, K. Ledingham, L. Robson, J. Yang, P. McKenna, T. McCanny, J. Melone, K. Amthor, F. Ewald, B. Liesfeld, H. Schwoerer, and R. Sauerbrey, "Study of photo-proton reactions driven by bremsstrahlung radiation of high-intensity laser generated electrons," New J. Phys. 10, 043037 (2008).
- ³³E. Brunetti, R. P. Shanks, G. G. Manahan, M. R. Islam, B. Ersfeld, M. P. Anania, S. Cipiccia, R. C. Issac, G. Raj, G. Vieux, G. H. Welsh, S. M. Wiggins, and D. A. Jaroszynski, "Low emittance, high brilliance relativistic electron beams from a laser-plasma accelerator," Phys. Rev. Lett. 105, 215007 (2010).
- ³⁴D. Habs, M. Günther, M. Jentschel, and W. Urban, "Refractive index of silicon at γ ray energies," Phys. Rev. Lett. 108, 184802 (2012).
- ³⁵Y. Glinec, J. Faure, L. Le Dain, S. Darbon, T. Hosokai, J. J. Santos, E. Lefebvre, J.-P. Rousseau, F. Burgy, B. Mercier, and V. Malka, "Highresolution γ-ray radiography produced by a laser-plasma driven electron source," Phys. Rev. Lett. 94, 025003 (2005).
- ³⁶Z.-H. Hu, X.-J. Wang, D.-X. Hui, Q.-T. Zhao, R. Cheng, Y.-T. Zhao, Z.-M. Zhang, and Y.-N. Wang, "Gamma-ray beam produced by a plasma lens focused electron bunch," Phys. Plasmas 27, 023103 (2020).
- ³⁷M. Fuchs, R. Weingartner, A. Popp, Z. Major, S. Becker, J. Osterhoff, I. Cortrie, B. Zeitler, R. Hörlein, G. D. Tsakiris, U. Schramm, T. P. Rowlands-Rees, S. M. Hooker, D. Habs, F. Krausz, S. Karsch, and F. Grüner, "Laser-driven soft-X-ray undulator source," Nat. Phys. 5, 826–829 (2009).
- ³⁸R. Weingartner, M. Fuchs, A. Popp, S. Raith, S. Becker, S. Chou, M. Heigoldt, K. Khrennikov, J. Wenz, T. Seggebrock, B. Zeitler, Z. Major, J. Osterhoff, F. Krausz, S. Karsch, and F. Grüner, "Imaging laser-wakefield-accelerated electrons using miniature magnetic quadrupole lenses," Phys. Rev. ST Accel. Beams 14, 052801 (2011).
- ³⁹M. P. Anania, E. Brunetti, S. M. Wiggins, D. W. Grant, G. H. Welsh, R. C. Issac, S. Cipiccia, R. P. Shanks, G. G. Manahan, C. Aniculaesei, S. B. van der Geer, M. J. de Loos, M. W. Poole, B. J. A. Shepherd, J. A. Clarke, W. A. Gillespie, A. M. MacLeod, and D. A. Jaroszynski, "An ultrashort pulse ultra-violet radiation undulator source driven by a laser plasma wakefield accelerator," Appl. Phys. Lett. 104, 264102 (2014).
- ⁴⁰G. Manahan, E. Brunetti, C. Aniculaesei, M. P. Anania, S. Cipiccia, M. Islam, D. Grant, A. Subiel, R. Shanks, R. Issac, G. Welsh, S. Wiggins, and D. Jaroszynski, "Characterization of laser-driven single and double electron bunches with a permanent magnet quadrupole triplet and pepper-pot mask," New J. Phys. 16, 103006 (2014).
- ⁴¹ J. K. Lim, P. Frigola, G. Travish, J. B. Rosenzweig, S. G. Anderson, W. J. Brown, J. S. Jacob, C. L. Robbins, and A. M. Tremaine, "Adjustable, short focal length permanent-magnet quadrupole based electron beam final focus system," Phys. Rev. ST Accel. Beams 8, 072401 (2005).
- ⁴² A. Ghaith, D. Oumbarek, C. Kitégi, M. Valléau, F. Marteau, and M.-E. Couprie, "Permanent magnet-based quadrupoles for plasma acceleration sources," Instruments 3, 27 (2019).
- ⁴³V. Yanovsky, V. Chvykov, G. Kalinchenko, P. Rousseau, T. Planchon, T. Matsuoka, A. Maksimchuk, J. Nees, G. Cheriaux, G. Mourou, and K. Krushelnick, "Ultra-high intensity-300-TW laser at 0.1 Hz repetition rate." Opt. Express 16, 2109–2114 (2008).
- ⁴⁴S. Agostinelli, J. Allison, K. a. Amako, J. Apostolakis, H. Araujo, P. Arce, M. Asai, D. Axen, S. Banerjee, G. Barrand, F. Behner, L. Bellagamba, J. Boudreau, L. Broglia, A. Brunengo, H. Burkhardt, S. Chauvie, J. Chuma, R. Chytracek, G. Cooperman, G. Cosmo, P. Degtyarenko, A. Dell'Acqua, G. Depaola, D. Dietrich, R. Enami, A. Feliciello, C. Ferguson, H. Fesefeldt, G. Folger, F. Foppiano, A. Forti, S. Garelli, S. Giani, R. Giannitrapani, D. Gibin, J. J. G. Cadenas, I. Gonzalez, G. G.

- Abril, G. Greeniaus, W. Greiner, V. Grichine, A. Grossheim, S. Guatelli, P. Gumplinger, R. Hamatsu, K. Hashimoto, H. Hasui, A. Heikkinen, A. Howard, V. Ivanchenko, A. Johnson, F. W. Jones, J. Kallenbach, N. Kanaya, M. Kawabata, *et al.*, "Geant4—a simulation toolkit," Nucl. Instrum. Methods Phys. Res., Sect. A **506**, 250–303 (2003).
- ⁴⁵T. Z. Zhao, K. Behm, C. F. Dong, X. Davoine, S. Y. Kalmykov, V. Petrov, V. Chvykov, P. Cummings, B. Hou, A. Maksimchuk, J. A. Nees, V. Yanovsky, A. G. R. Thomas, and K. Krushelnick, "High-flux femtosecond x-ray emission from controlled generation of annular electron beams in a laser wakefield accelerator," Phys. Rev. Lett. 117, 094801 (2016).

⁴⁶K. Behm, A. Hussein, T. Z. Zhao, S. Dann, B. X. Hou, V. Yanovsky, J. Nees, A. Maksimchuk, W. Schumaker, A. Thomas, and K. Krushelnick, "Measurements of electron beam ring structures from laser wakefield accelerators," Plasma Phys. Controlled Fusion 61, 065012 (2019).

- ⁴⁷A. Maitrallain, E. Brunetti, M. Streeter, B. Kettle, R. Spesyvtsev, G. Vieux, M. Shahzad, B. Ersfeld, S. R. Yoffe, A. Kornaszewski, O. Finlay, Y. Ma, F. Albert, N. Bourgeois, S. J. D. Dann, N. Lemos, S. Cipiccia, J. M. Cole, I. G. González, L. Willingale, A. Higginbotham, A. E. Hussein, M. Šmid, K. Falk, K. Krushelnick, N. C. Lopes, E. Gerstmayr, C. Lumsdon, O. Lundh, S. P. D. Mangles, Z. Najmudin, P. P. Rajeev, D. R. Symes, A. G. R. Thomas, and D. A. Jaroszynski, "Parametric study of high-energy ring-shaped electron beams from a laser wakefield accelerator," New J. Phys. 24, 013017 (2022).
- ⁴⁸M. J. Berger, J. S. Coursey, M. A. Zucker, and J. Chang, "ESTAR, PSTAR, and ASTAR: computer programs for calculating stopping-power and range tables for electrons, protons, and helium ions (version 1.2.3)," (National Institute of Standards and Technology, Gaithersburg, MD, 2005).
- ⁴⁹A. Hannasch, A. L. Garcia, M. LaBerge, R. Zgadzaj, A. Koehler, J. P. Cabadag, O. Zarini, T. Kurz, A. Ferrari, M. Molodtsova, L. Naumann, T. E. Cowan, U. Schramm, A. Irman, and M. C. Downer, "Compact spectroscopy of keV to MeV X-rays from a laser wakefield accelerator," Sci. Rep 11, 1–16 (2021).
- ⁵⁰P. L. Shkolnikov, A. E. Kaplan, A. Pukhov, and J. Meyer-ter Vehn, "Positron and gamma-photon production and nuclear reactions in cascade processes initiated by a sub-terawatt femtosecond laser," Appl. Phys. Lett. 71, 3471–3473 (1997).
- ⁵¹H. N. Mülthei and B. Schorr, "On an iterative method for the unfolding of spectra." Nucl. Instrum. Methods Phys. Res. A 257, 371–377 (1987).
- ⁵²D. J. S. Findlay, "Analytic representation of bremsstrahlung spectra from thick radiators as a function of photon energy and angle," Nucl. Instrum. Methods Phys. Res. A 276, 598–601 (1989).
- ⁵³T. Bonnet, M. Comet, D. Denis-Petit, F. Gobet, F. Hannachi, M. Tarisien, M. Versteegen, and M. Aléonard, "Response functions of imaging plates to photons, electrons and 4he particles," Rev. Sci. Instrum. 84, 103510 (2013).
- ⁵⁴A. Alejo, G. M. Samarin, J. R. Warwick, and G. Sarri, "Laser-wakefield

- electron beams as drivers of high-quality positron beams and inverse-compton-scattered photon beams," Front. Phys. 7, 49 (2019).
- ⁵⁵D. Habs and U. Köster, "Production of medical radioisotopes with high specific activity in photonuclear reactions with γ-beams of high intensity and large brilliance," Appl. Phys. B 103, 501–519 (2011).
- ⁵⁶R. Takashima, M. Todoriki, S. Hasegawa, K. Nemoto, and K. Kato, "Numerical evaluation of nuclide analysis of I 129, Sr 90, and Cs 137 using bremsstrahlung high energy x ray generated by ultrashort pulse laser," J. Appl. Phys. 100, 064906 (2006).
- ⁵⁷G. Sarri, K. Poder, J. M. Cole, W. Schumaker, A. Di Piazza, B. Reville, T. Dzelzainis, D. Doria, L. A. Gizzi, G. Grittani, S. Kar, C. H. Keitel, K. Krushelnick, S. Kuschel, S. P. D. Mangles, Z. Najmudin, N. Shukla, L. O. Silva, D. Symes, A. G. R. Thomas, M. Vargas, J. Vieira, and M. Zepf, "Generation of neutral and high-density electron–positron pair plasmas in the laboratory," Nat. Commun. 6, 1–8 (2015).
- ⁵⁸J. Warwick, T. Dzelzainis, M. E. Dieckmann, W. Schumaker, D. Doria, L. Romagnani, K. Poder, J. M. Cole, A. Alejo, M. Yeung, K. Krushelnick, S. P. D. Mangles, Z. Najmudin, B. Reville, G. M. Samarin, D. D. Symes, A. G. R. Thomas, M. Borghesi, and G. Sarri, "Experimental observation of a current-driven instability in a neutral electron-positron beam," Phys. Rev. Lett. 119, 185002 (2017).
- ⁵⁹A. Gruzinov, "Gamma-ray burst phenomenology, shock dynamo, and the first magnetic fields," Astrophys. J. **563**, L15 (2001).
- ⁶⁰P. Chang, A. Spitkovsky, and J. Arons, "Long-term evolution of magnetic turbulence in relativistic collisionless shocks: electron-positron plasmas," Astrophys. J. **674**, 378 (2008).
- ⁶¹H. Chen, F. Fiuza, A. Link, A. Hazi, M. Hill, D. Hoarty, S. James, S. Kerr, D. D. Meyerhofer, J. Myatt, J. Park, Y. Sentoku, and G. J. Williams, "Scaling the yield of laser-driven electron-positron jets to laboratory astrophysical applications," Phys. Rev. Lett. 114, 215001 (2015).
- ⁶²D. Pellicciotta, F. Frontera, G. Loffredo, A. Pisa, K. Andersen, P. Courtois, B. Hamelin, V. Carassiti, M. Melchiorri, and S. Squerzanti, "Laue lens development for hard X-rays (> 60 kev)," IEEE Trans. Nucl. Sci. 53, 253–258 (2006).
- ⁶³J. Van Tilborg, S. Steinke, C. G. R. Geddes, N. H. Matlis, B. H. Shaw, A. J. Gonsalves, J. V. Huijts, K. Nakamura, J. Daniels, C. Schroeder, C. Benedetti, E. Esarey, S. S. Bulanov, N. A. Bobrova, P. V. Sasorov, and W. P. Leemans, "Active plasma lensing for relativistic laser-plasma-accelerated electron beams," Phys. Rev. Lett. 115, 184802 (2015).
- ⁶⁴T. Yang, H. Cheng, Y. Yan, M. Wu, D. Li, Y. Li, Y. Xia, C. Lin, and X. Yan, "Designing of active plasma lens for focusing laser-plasma-accelerated pulsed proton beams," Phys. Rev. Accel. Beams 24, 031301 (2021).
- ⁶⁵C. A. Lindstrøm, E. Adli, G. Boyle, R. Corsini, A. E. Dyson, W. Farabolini, S. M. Hooker, M. Meisel, J. Osterhoff, J.-H. Röckemann, L. Schaper, and K. N. Sjobak, "Emittance preservation in an aberration-free active plasma lens," Phys. Rev. Lett. 121, 194801 (2018).